Giant magnetothermopower of magnon-assisted transport in ferromagnetic tunnel junctions

Edward McCann and Vladimir I. Fal'ko
Department of Physics, Lancaster University, Lancaster, LA1 4YB, United Kingdom
and Grenoble High Magnetic Field Laboratory, MPI/FKF and CNRS, BP 166, F-38042 Grenoble Cedex 9, France
(Received 1 May 2002; published 30 October 2002)

We present a theoretical description of the thermopower due to magnon-assisted tunneling in a mesoscopic tunnel junction between two ferromagnetic metals. The thermopower is generated in the course of thermal equilibration between two baths of magnons, mediated by electrons. For a junction between two ferromagnets with antiparallel polarizations, the ability of magnon-assisted tunneling to create thermopower S_{AP} depends on the difference between the size $\Pi_{\uparrow,\downarrow}$ of the majority- and minority-band Fermi surfaces and it is proportional to a temperature-dependent factor $(k_BT/\omega_D)^{3/2}$ where ω_D is the magnon Debye energy. The latter factor reflects the fractional change in the net magnetization of the reservoirs due to thermal magnons at temperature T (Bloch's $T^{3/2}$ law). In contrast, the contribution of magnon-assisted tunneling to the thermopower S_P of a junction with parallel polarizations is negligible. As the relative polarizations of ferromagnetic layers can be manipulated by an external magnetic field, a large difference $\Delta S = S_{AP} - S_P \approx S_{AP} \sim -(k_B/e) f(\Pi_\uparrow, \Pi_\downarrow) \times (k_BT/\omega_D)^{3/2}$ results in a magnetothermopower effect. This magnetothermopower effect becomes giant in the extreme case of a junction between two half-metallic ferromagnets, $\Delta S \sim -k_B/e$.

DOI: 10.1103/PhysRevB.66.134424 PACS number(s): 72.25.−b, 72.15.Jf, 73.40.Rw, 73.23.−b

I. INTRODUCTION

Spin-polarized transport has recently been the subject of intense theoretical and experimental interest.[1] The mismatch of spin currents at the interface between two ferromagnetic (F) electrodes with antiparallel spin polarizations produces a larger contact resistance than a junction with parallel polarizations, leading to tunneling magnetoresistance in F-F junctions[2,3] and giant magnetoresistance (GMR) in multilayer structures.[4,5] Systems displaying GMR have shown other magnetotransport effects including substantial magnetothermopower[6–15] with a strong temperature dependence. Thermoelectric effects have also been discussed in the context of spin injection across a ferromagnetic-paramagnetic junction.[16]

The Mott formula[17] $S = -(\pi^2 k_B^2 T/3e)(\partial \ln \sigma(\epsilon)/\partial \epsilon)_{\epsilon_F}$ relates the thermopower S of a system to the derivative with respect to energy of the electrical conductivity, $\sigma(\epsilon)$, near the Fermi energy ϵ_F so that, in metals, S typically contains a small parameter such as k_BT/ϵ_F. In magnetic multilayers with highly transparent interfaces, the Mott formula has been used as a basis for theories of transport that explain the origin of the magnetothermopower effect as due to either the difference in the energy dependence of the density of states for majority- and minority-spin bands in ferromagnetic layers[13,18] or a different efficiency of electron-magnon scattering for carriers in opposite spin states.[8] In particular, the electron-magnon interaction in a ferromagnetic layer was incorporated to explain the observation[8] of a strong temperature dependence of $S(T)$ and gave, theoretically, a much larger thermopower in the parallel configuration of multilayers with highly transparent interfaces than in the antiparallel one, $S_P \gg S_{AP}$. For tunnel junctions, magnon-assisted processes have been studied both theoretically[19] and experimentally[20] with a view to relate nonlinear $I(V)$ characteristics to the density of states of magnons $\Omega(\omega)$ as $d^2I/dV^2 \propto \Omega(eV)$.

In this paper we investigate a model of the electron-magnon interaction assisted thermopower in a mesoscopic size ferromagnet/insulator/ferromagnet tunnel junction, which yields a different prediction. The bottleneck of both charge and heat transport lies in a small-area tunnel contact between ferromagnetic metals held at different temperatures. The thermopower is generated in the course of thermal equilibration between two baths of magnons as mediated by electrons, and in the relatively high resistance antiparallel (AP) configuration of a ferromagnetic tunnel junction, it depends on the difference between the size of the majority- and minority-band Fermi surfaces. For a momentum-conserving tunneling model we find that

$$S_{AP} \approx -\frac{k_B}{e}\frac{(\Pi_+ - \Pi_-)}{2\Pi_-}\,\delta m(T), \tag{1}$$

$$\delta m(T) = \frac{3.47}{\xi}\left(\frac{k_BT}{\omega_D}\right)^{3/2}, \tag{2}$$

where Π_+ (Π_-) is the area of the maximal cross section of the Fermi surface of majority (minority) electrons in the plane parallel to the interface ($\Pi_+ > \Pi_-$). The function $\delta m(T)$ is the fractional change in the magnetization of the reservoirs due to thermal magnons at temperature T (Bloch's $T^{3/2}$ law), ξ is the spin of localized moments, and ω_D is the magnon Debye energy. On the other hand, we find that the contribution of magnon-assisted tunneling to the thermopower of a parallel configuration is negligible.

As an extreme example, the magnetothermopower effect is most pronounced in the case of half-metallic ferromagnets, where the exchange spin splitting Δ between the majority and minority conduction bands is greater than the Fermi energy ϵ_F measured from the bottom of the majority band and the Fermi density of states in the minority band is zero. In the antiparallel configuration of such a junction, where the emission or absorption of a magnon would lift the spin blockade of electronic transfer between ferromagnetic met-

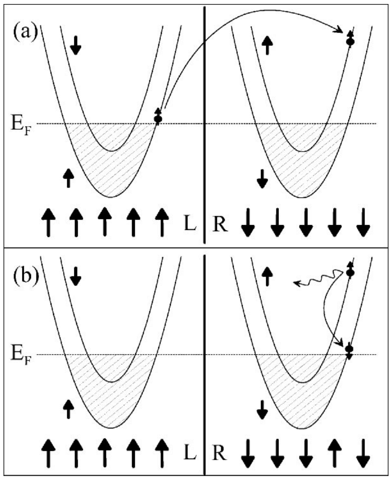

FIG. 1. Schematic of magnon-assisted tunneling via an intermediate minority state. This example shows a transition from an initial majority state on the left to a final majority state on the right across a junction in an antiparallel configuration. (a) The process begins with a spin-up majority electron on the left, which then tunnels through the barrier (without spin flip) into an intermediate, virtual state with spin-up minority polarization on the right. (b) The electron emits a magnon (wavy line) and incorporates itself into a previously unoccupied state in the spin-down majority band on the right.

als, we predict a large thermopower effect, whereas in the lower-resistance parallel configuration thermopower is relatively weak[21]:

$$S_{AP} \approx -0.64\frac{k_B}{e}, \quad \frac{S_P}{S_{AP}} \sim \frac{k_B T}{\epsilon_F}. \tag{3}$$

This is because the contribution of magnon-assisted transport to the thermopower in the parallel configuration S_P is zero and the thermopower only arises from the energy dependence of the electronic density of states near the Fermi energy.

The magnon-assisted processes that we consider are similar to those discussed in Ref. 19 in relation to the magnon contribution to the nonlinear conductance. In a ferromagnetic tunnel junction in the antiparallel configuration, the elastic contribution to the conductance is suppressed by the mismatch of spin currents at the interface. However, it is possible to lift spin current blockade while conserving the overall spin of the system by emitting or absorbing magnons. For example, the change of spin that occurs when a minority carrier flips and occupies a majority state is compensated for by an opposite change of spin due to magnon emission. As a result, the spin current carried by electrons crossing an interface between oppositely polarized ferromagnets is carried further by the flow of magnons (spin waves).

Microscopically, a typical magnon-assisted process that contributes to the thermopower in the antiparallel configuration, Eqs. (1) and (3), is shown schematically in Fig. 1. Here the majority electrons on the left-hand side of the junction are "spin up" and the majority electrons on the right are "spin down." The transition begins with a spin-up majority electron on the left, which then tunnels through the barrier (without spin flip) into an intermediate, virtual state with spin-up minority polarization on the right [Fig. 1(a)]. In the final step, Fig. 1(b), the electron emits a magnon and incorporates itself into a previously unoccupied state in the spin-down majority band on the right. In our approach, we take into account such inelastic tunneling processes that involve magnon emission and absorption on both sides of the interface, as well as elastic electron transfer processes, in order to obtain a balance equation for the current $I(V,\Delta T)$ as a function of bias voltage V and of the temperature drop ΔT. In the linear response regime the electrical current may be written as

$$I = G_V V + G_{\Delta T}\Delta T, \tag{4}$$

where G_V is the electrical conductance and $G_{\Delta T}$ is a thermoelectric coefficient describing the response to a temperature difference. Under conditions of zero net current, the thermopower coefficient is

$$S = -\frac{V}{\Delta T} = \frac{G_{\Delta T}}{G_V}. \tag{5}$$

The paper is organized as follows. In Sec. II we introduce the model and technique used for describing a tunnel junction and we calculate the thermopower in the AP configuration. We present a detailed description of two different models of the interface: a uniformly transparent interface where the component of momentum parallel to the interface is conserved and a randomly transparent interface. In Sec. III we demonstrate that the contribution of magnon-assisted tunneling to the thermopower of a parallel (P) configuration is negligible. In Sec. IV we discuss the magnetothermopower, give an order of magnitude estimate of the size of the effect, and present results for the magnetothermopower of a junction between two half-metallic ferromagnets.

II. THERMOPOWER OF AN ANTIPARALLEL JUNCTION

A. Description of the model

Our initial aim is to write a balance equation for the current in terms of occupation numbers of electrons $n_{L(R)}(\epsilon_{\mathbf{k}\alpha}) = \{\exp[(\epsilon_{\mathbf{k}\alpha} - \epsilon_F^{L(R)})/(k_B T_{L(R)})]+1\}^{-1}$ and of magnons $N_{L(R)}(\mathbf{q}) = \{\exp[\omega_{\mathbf{q}}/(k_B T_{L(R)})]-1\}^{-1}$ on the left- (right-) hand side of the junction, where $T_{L(R)}$ is the temperature on the left- (right-) hand side, $\epsilon_F^L - \epsilon_F^R = -eV$, and $\omega_{\mathbf{q}}$ is the energy of a magnon of wave vector $\mathbf{q}$. In the following we set $T_L = T$ and $T_R = T - \Delta T$ and we shall speak throughout in terms of the transfer of electrons with charge $-e$. The index $\alpha = \{+,-\}$ takes account of the splitting of conduction band electrons into majority $\epsilon_{\mathbf{k}+}$ and minority $\epsilon_{\mathbf{k}-}$ subbands, $\epsilon_{\mathbf{k}\alpha} = \epsilon_{\mathbf{k}} - \alpha\Delta/2$, where $\epsilon_{\mathbf{k}}$ is the bare electron energy and Δ is the spin splitting energy.

In an AP junction, we assume that the majority electrons on the left-hand side of the junction are "spin up" and the majority electrons on the right are "spin down." The total Hamiltonian of the system is

$$H = H_F^L + H_F^R + H_T, \tag{6}$$

$$H_T=\sum_{\mathbf{k}\mathbf{k}'\alpha}[t_{\mathbf{k},\mathbf{k}'}c^{\dagger}_{\mathbf{k}\alpha}c_{\mathbf{k}'\bar{\alpha}}+t^{*}_{\mathbf{k},\mathbf{k}'}c^{\dagger}_{\mathbf{k}'\bar{\alpha}}c_{\mathbf{k}\alpha}], \tag{7}$$

where H_T is the tunneling Hamiltonian,[22–24] which is written in terms of creation and annihilation Fermi operators $c^{\dagger}$ and c. Here $\bar{\alpha}\equiv-\alpha$ and we assume that spin is conserved when an electron tunnels across the interface. The tunneling matrix elements $t_{\mathbf{k},\mathbf{k}'}$ describe the transfer of an electron with wave vector $\mathbf{k}$ on the left to the state with $\mathbf{k}'$ on the right. We will consider $t_{\mathbf{k},\mathbf{k}'}$ to be a symmetric matrix of the form

$$t_{\mathbf{k},\mathbf{k}'}=\tilde{t}_{\mathbf{k}_{\|},\mathbf{k}'_{\|}}\left|\frac{h^2 v_L^z(\mathbf{k})v_R^z(\mathbf{k}')}{L^2}\right|^{1/2}, \tag{8}$$

where $v^z_{L,R}(\mathbf{k})=\partial\epsilon_{L,R}(\mathbf{k})/\partial(\hbar k_z)$ are components of electron velocity perpendicular to the interface and $\epsilon_{L,R}(\mathbf{k})$ denotes the electron energy dispersion in the electrodes. In our model for t, we neglect its explicit energy dependence. However, $\tilde{t}_{\mathbf{k}_{\|},\mathbf{k}'_{\|}}$ can describe both clean and diffusive interfaces by taking into account the conservation of $\mathbf{k}_{\|}$, the component of momentum parallel to the interface.

The term $H_F^{L(R)}$ is the Hamiltonian of the ferromagnetic electrode on the left (right) side of the junction in the absence of tunneling. We use the so called s-f (s-d) model,[25,26] which assumes that magnetism and electrical conduction are caused by different groups of electrons that are coupled via an intra-atomic exchange interaction, although we note that the same results, in the lowest order of electron-magnon interactions, may be obtained from a model of itinerant ferromagnets.[27] The magnetism originates from inner atomic shells (e.g., d or f) which have unoccupied electronic orbitals and, therefore, possess magnetic moments whereas the conduction is related to electrons with delocalized wave functions. Using the Holstein-Primakoff transformation[28] the operators of the localized moments in the interaction Hamiltonian can be expressed via magnon creation and annihilation operators $b^{\dagger},b$. At low temperatures, where the average number of magnons is small $\langle b^{\dagger}b\rangle\ll 2\xi$ (ξ is the spin of the localized moments), the Hamiltonian of the ferromagnet $H_F^{L(R)}$ can be written as follows:

$$H_F^{L(R)}=H_e^{L(R)}+H_m^{L(R)}+H_{em}^{L(R)}, \tag{9}$$

$$H_e^{L(R)}=\sum_{\mathbf{k}\alpha}\epsilon_{\mathbf{k}\alpha}c^{\dagger}_{\mathbf{k}\alpha}c_{\mathbf{k}\alpha}, \quad \epsilon_{\mathbf{k}\alpha}=\epsilon_{\mathbf{k}}-\alpha\Delta/2, \tag{10}$$

$$H_m^{L(R)}=\sum_{\mathbf{q}}\omega_{\mathbf{q}}b^{\dagger}_{\mathbf{q}}b_{\mathbf{q}}, \quad \omega_{q=0}=\omega_0, \tag{11}$$

$$H_{em}^{L(R)}=-\frac{\Delta}{\sqrt{2\xi\mathcal{N}}}\sum_{\mathbf{k}\mathbf{q}}[c^{\dagger}_{\mathbf{k}-\mathbf{q}+}c_{\mathbf{k}-}b^{\dagger}_{\mathbf{q}}+c^{\dagger}_{\mathbf{k}-}c_{\mathbf{k}-\mathbf{q}+}b_{\mathbf{q}}]. \tag{12}$$

The first term $H_e^{L(R)}$, Eq. (10), deals with conduction band electrons which are split into majority $\epsilon_{\mathbf{k}+}$ and minority $\epsilon_{\mathbf{k}-}$ subbands due to s-f (s-d) exchange. The Hamiltonian $H_m^{L(R)}$, Eq. (11), describes free magnons with spectrum ω_q which in the general case has a gap $\omega_{q=0}=\omega_0$. The third term $H_{em}^{L(R)}$, Eq. (12), is the electron-magnon coupling resulting from the intra-atomic exchange interaction between the spins of the conduction electrons and the localized moments.

The calculation is performed using standard second-order perturbation theory.[29] We write the total Hamiltonian, Eq. (6), as $H=H_0+V$, where the perturbation $V=H_T+H^L_{em}+H^R_{em}$ is the sum of the tunneling Hamiltonian and the electron-magnon interactions in the electrodes. First-order terms provide an elastic contribution to the current that do not involve any change of the spin orientation of the itinerant electrons, while second-order terms account for inelastic, magnon-assisted processes.

B. Elastic contribution to the current

The first-order contribution to the current, in antiparallel configuration, arises from elastic tunneling without any spin flip between a majority conduction electron state on one side of the junction and a minority state on the other. Consider for example an initial state consisting of an additional majority spin-up electron on the left with wave vector $\mathbf{k}_L$ and energy $\epsilon_{\mathbf{k}_L+}$. This electron can tunnel, with matrix element t^{*}_{LR}, into a minority spin up state on the right with wave vector $\mathbf{k}_R$ and energy $\epsilon_{\mathbf{k}_R-}$. In addition there is a second process which is a transition between the same two states, but in the reverse order, giving a contribution to the current with an opposite sign. Together, the two processes give a balance equation for the first-order contribution to the current between the majority band on the left and the minority on the right. In addition, there are two first-order processes that result in transitions between the minority band on the left and the majority on the right. Overall, the first-order contribution to the current is $I^{(1)}_{AP}$ where

$$\begin{aligned}I^{(1)}_{AP}=&-4\pi^2\frac{e}{h}\int_{-\infty}^{+\infty}d\epsilon\sum_{\mathbf{k_L}\mathbf{k_R}}\sum_{\alpha=\{\pm\}}|t_{\mathbf{k_L},\mathbf{k_R}}|^2\delta(\epsilon-\epsilon_{\mathbf{k_L}\alpha})\\&\times\delta(\epsilon-eV-\epsilon_{\mathbf{k_R}\bar{\alpha}})\{n_L(\epsilon_{\mathbf{k_L}\alpha})[1-n_R(\epsilon_{\mathbf{k_R}\bar{\alpha}})]\\&-[1-n_L(\epsilon_{\mathbf{k_L}\alpha})]n_R(\epsilon_{\mathbf{k_R}\bar{\alpha}})\},\end{aligned} \tag{13}$$

and $\bar{\alpha}\equiv-\alpha$. Neglecting terms that contain the small parameter k_BT/ϵ_F, the current may be written as

$$I^{(1)}_{AP}\approx\frac{e^2}{h}V(\mathcal{T}_{+-}+\mathcal{T}_{-+}). \tag{14}$$

For convenience we have grouped all information about the nature of the interface into a parameter $\mathcal{T}_{\alpha\alpha'}$,

$$\mathcal{T}_{\alpha\alpha'}\approx4\pi^2\sum_{\mathbf{k_L}\mathbf{k_R}}|t_{\mathbf{k_L},\mathbf{k_R}}|^2\delta(\epsilon-\epsilon_{\mathbf{k_L}\alpha})\delta(\epsilon-\epsilon_{\mathbf{k_R}\alpha'}), \tag{15}$$

which is equivalent to the sum over all scattering channels, between spin states α on the left and α' on the right, of the transmission eigenvalues usually introduced in the Landauer formula,[30–32] although we restrict ourselves to the tunneling regime in this paper. Later we will employ models of two

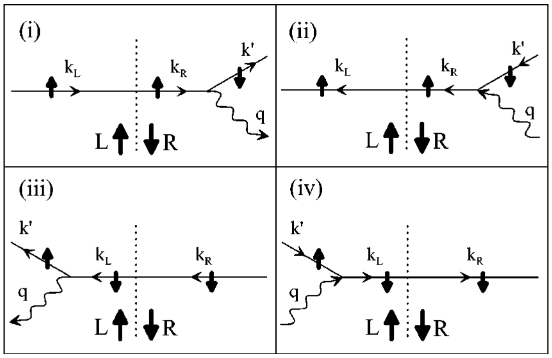

FIG. 2. Schematic of four electron-type processes, across a junction in the antiparallel configuration, which involve transitions from majority initial to majority final states via a virtual intermediate state in the minority band: (i) and (iii) involve magnon emission on the right and left hand sides, respectively, whereas (ii) and (iv) involve magnon absorption on the right and left.

types of interface explicitly: a uniformly transparent interface where the component of momentum parallel to the interface is conserved and a randomly transparent interface.

C. Magnon-assisted contribution to the current

Below we describe processes which contribute to magnon-assisted tunneling. For convenience, we divide them into two groups that we label as "electron" and "hole" processes. In electron processes, an increase in the number of magnons in one electrode is achieved by accepting electrons from the other electrode whereas, in hole processes, an increase in the number of magnons in one electrode is achieved by injecting electrons into the other electrode.

The electron processes are shown schematically in Fig. 2. The straight lines show the direction of electron transfer, whereas the wavy lines denote the emission or absorption of magnons. The processes are drawn using the rule, appropriate for ferromagnetic electron-magnon exchange, that an electron in a minority state scatters into a majority state by emitting a magnon. The electron processes in Fig. 2 involve transitions from majority initial states to majority final states via an intermediate, virtual state in the minority band. For example, process (i), which is the same as the process shown in more detail in Fig. 1, begins with a spin-up majority electron on the left with wave vector $\mathbf{k}_L$ and energy $\epsilon_{\mathbf{k}_L+}$. Then, this electron tunnels across the barrier (without spin flip) to occupy a virtual, intermediate state with wave vector $\mathbf{k}_R$ in the spin-up minority band on the right as depicted in the right part of Fig. 1(a) with energy $\epsilon_{\mathbf{k}_R-}$. The energy difference between the states is $\epsilon_{\mathbf{k}_R}-\epsilon_{\mathbf{k}_L}+\Delta$ so that the matrix element for the transition contains an energy in the denominator related to the inverse lifetime of the electron in the virtual state. For $k_BT,eV\ll\Delta$, when both initial and final electron states should be taken close to the Fermi level, only long-wavelength magnons can be emitted, so that the energy deficit in the virtual states can be approximated as $\epsilon_{\mathbf{k_R}}-\epsilon_{\mathbf{k_L}}+\Delta\approx\Delta$. As noticed in Refs. 25,33, and 34, this cancels out the large exchange parameter since the same electron-core spin-exchange constant appears both in the splitting between minority and majority bands and in the electron-magnon coupling.

The second part of the transition is sketched in Fig. 1(b) where the electron in the virtual minority spin-up state incorporates itself into a state in the majority spin-down band on the right by emitting a magnon, which is shown as a flip of one of the localized moments. The wave vector of the electron in the final state is $\mathbf{k}'$ and the total energy of the final (many-body) state is $\epsilon_{\mathbf{k}'+}-\omega_{\mathbf{q}}$. Similar considerations enable us to write down the contribution to the current from all the electron processes in Fig. 2. We group the processes into pairs which involve transitions between the same series of states, but in the opposite time order so that they give a current with different signs; hence their sum gives a balance equation. The contributions to the current of the processes (i) and (ii), labeled as $I_{AP}^{(\mathrm{i,ii})}$, are given by

$$I_{AP}^{(\mathrm{i,ii})}=-4\pi^2\frac{e}{h}\int_{-\infty}^{+\infty}d\epsilon\sum_{\mathbf{k_L}\mathbf{k}'\mathbf{q}}\frac{|t_{\mathbf{k_L},\mathbf{k}'}|^2}{2\xi\mathcal{N}}\delta(\epsilon-\epsilon_{\mathbf{k_L}+})\times\delta(\epsilon-eV-\epsilon_{\mathbf{k}'+}-\omega_{\mathbf{q}})\{n_L(\epsilon_{\mathbf{k_L}+})[1-n_R(\epsilon_{\mathbf{k}'+})]\times[1+N_R(\mathbf{q})]-[1-n_L(\epsilon_{\mathbf{k_L}+})]n_R(\epsilon_{\mathbf{k}'+})N_R(\mathbf{q})\},\tag{16}$$

where $\mathbf{q}=\mathbf{k_R}-\mathbf{k}'$. The processes (iii) and (iv) are similar to processes (i) and (ii), respectively, except that electrons interact with magnons in the left electrode:

$$I_{AP}^{(\mathrm{iii,iv})}=-4\pi^2\frac{e}{h}\int_{-\infty}^{+\infty}d\epsilon\sum_{\mathbf{k}'\mathbf{k_R}\mathbf{q}}\frac{|t_{\mathbf{k}',\mathbf{k_R}}|^2}{2\xi\mathcal{N}}\delta(\epsilon-eV-\epsilon_{\mathbf{k_R}+})\times\delta(\epsilon-\epsilon_{\mathbf{k}'+}-\omega_{\mathbf{q}})\{-n_R(\epsilon_{\mathbf{k_R}+})[1-n_L(\epsilon_{\mathbf{k}'+})]\times[1+N_L(\mathbf{q})]+[1-n_R(\epsilon_{\mathbf{k_R}+})]n_L(\epsilon_{\mathbf{k}'+})N_L(\mathbf{q})\},\tag{17}$$

where $\mathbf{q}=\mathbf{k_L}-\mathbf{k}'$. Energies on the right are shifted by eV to take account of the voltage difference across the junction.

An example of a hole process is shown in detail in Figs. 3(a) and 3(b), and Fig. 3(c) shows the same process, (v), plus other hole processes (vi), (vii), and (viii). The hole processes involve transitions from minority initial to minority final states via a virtual intermediate state in the majority band. In contrast to the electron processes, an increase in the number of magnons in one electrode is achieved by injecting electrons into the other electrode. As an example we describe in detail the calculation of the matrix element for process (v) shown in Figs. 3(a) and 3(b). The initial state has an additional spin-down minority electron near the Fermi level on the left [left part of Fig. 3(a)] with wave vector $\mathbf{k}_L$. The first step in the transition is the creation of an empty state below the Fermi level in the spin-down majority band on the right with wave vector $\mathbf{k}_R$ by the absorption of a magnon, wave vector $\mathbf{q}$, to elevate a spin-down majority electron up to a spin-up minority state above the Fermi level on the right with wave vector $\mathbf{k}'$ [right part of Fig. 3(a)]. The second part of the transition is sketched in Fig. 3(b) where the spin-down minority electron on the left tunnels across the barrier (without spin flip) to occupy the empty spin-down majority state

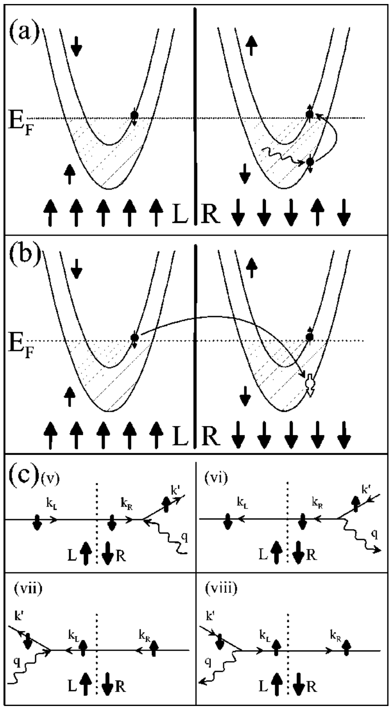

FIG. 3. Schematic of hole-type processes of magnon-assisted tunneling from an initial minority state to a final minority state via an intermediate majority state. (a) A typical process begins with the absorption of a magnon (wavy line) to elevate a spin-down majority electron below the Fermi level E_F on the right up to a spin-up minority state above E_F, creating an empty state below E_F in the spin-down majority band. (b) A spin-down minority electron on the left tunnels across the barrier (without spin flip) to occupy the empty spin-down majority state on the right. (c) The same process (v) plus remaining hole processes: (v) and (vii) involve magnon absorption on the right and left hand sides, respectively, whereas (vi) and (viii) involve magnon emission on the right and left.

on the right. The contributions to the current from processes (v) and (vi), $I_{AP}^{(\mathrm{v,vi})}$, and from processes (vii) and (viii), $I_{AP}^{(\mathrm{vii,viii})}$, are

$$
\begin{aligned}
I_{AP}^{(\mathrm{v,vi})}=&-4\pi^2\frac{e}{h}\int_{-\infty}^{+\infty}d\epsilon\sum_{\mathbf{k_L k' q}}\frac{|t_{\mathbf{k_L},\mathbf{k'}}|^2}{2\xi\mathcal{N}}\,\delta(\epsilon-\epsilon_{\mathbf{k_L}-})\\
&\times\delta(\epsilon-eV-\epsilon_{\mathbf{k'}-}+\omega_{\mathbf{q}})\\
&\times\{n_L(\epsilon_{\mathbf{k_L}-})[1-n_R(\epsilon_{\mathbf{k'}-})]N_R(\mathbf{q})\\
&-[1-n_L(\epsilon_{\mathbf{k_L}-})]n_R(\epsilon_{\mathbf{k'}-})[1+N_R(\mathbf{q})]\},
\end{aligned}
\tag{18}
$$

$$
\begin{aligned}
I_{AP}^{(\mathrm{vii,viii})}=&-4\pi^2\frac{e}{h}\int_{-\infty}^{+\infty}d\epsilon\sum_{\mathbf{k' k_R q}}\frac{|t_{\mathbf{k'},\mathbf{k_R}}|^2}{2\xi\mathcal{N}}\\
&\times\delta(\epsilon-eV-\epsilon_{\mathbf{k_R}-})\quad\delta(\epsilon-\epsilon_{\mathbf{k'}-}+\omega_{\mathbf{q}})\\
&\times\{-n_R(\epsilon_{\mathbf{k_R}-})[1-n_L(\epsilon_{\mathbf{k'}-})]N_L(\mathbf{q})\\
&+[1-n_R(\epsilon_{\mathbf{k_R}-})]n_L(\epsilon_{\mathbf{k'}-})[1+N_L(\mathbf{q})]\},
\end{aligned}
\tag{19}
$$

To make our analysis transparent, we rewrite the magnon-assisted current as the sum of two parts,

$$
I_{AP}=I_{AP}^{(\mathrm{i,ii})}+I_{AP}^{(\mathrm{iii,iv})}+I_{AP}^{(\mathrm{v,vi})}+I_{AP}^{(\mathrm{vii,viii})}=I_{AP}^{\mathrm{spont}}+I_{AP}^{\mathrm{stim}},
$$

the first of which, labeled I_{AP}^{spont}, does not contain any magnon occupation numbers and represents spontaneous emission processes,

$$
\begin{aligned}
I_{AP}^{\mathrm{spont}}=&-\frac{e}{h}\frac{(\mathcal{T}_{++}+\mathcal{T}_{--})}{2\xi\mathcal{N}}\int_{-\infty}^{+\infty}d\epsilon\int_0^{\infty}d\omega\ \Omega(\omega)\\
&\times\{n_L(\epsilon)[1-n_R(\epsilon-eV-\omega)]\\
&-[1-n_L(\epsilon-\omega)]n_R(\epsilon-eV)\},
\end{aligned}
\tag{20}
$$

where $\Omega(\omega)=\Sigma_{\mathbf{q}}\delta(\omega-\omega_{\mathbf{q}})$ is the magnon density of states that we assume to be the same on both sides of the junction. Since our main aim is to demonstrate the existence of an effect, we choose the simple example of a bulk, three-dimensional magnon density of states. We assume a quadratic magnon dispersion $\omega_q=Dq^2$ and apply the Debye approximation with a maximum magnon energy $\omega_D=D(6\pi^2/v)^{2/3}$ where v is the volume of a unit cell. This enables us to express the magnon density of states as $\Omega(\omega)=(3/2)\mathcal{N}\omega^{1/2}/\omega_D^{3/2}$. The term I_{AP}^{spont} is only nonzero for finite voltage. We calculate it in two different limits, the small temperature difference $\Delta T\ll T$ and large temperature difference $\Delta T=T, T_R=0$:

$$
\begin{aligned}
I_{AP}^{\mathrm{spont}}=&\frac{e^2}{h}\frac{V}{\xi}(\mathcal{T}_{++}+\mathcal{T}_{--})\left(\frac{k_BT_L}{\omega_D}\right)^{3/2}\frac{3}{4}\Gamma\left(\frac{3}{2}\right)\zeta\left(\frac{3}{2}\right)\\
&\times\begin{cases}1, & \Delta T\ll T,\\ 2-\sqrt{2}, & \Delta T=T,\end{cases}
\end{aligned}
\tag{21}
$$

where $\Gamma(x)$ is the gamma function and $\zeta(x)$ is Riemann's zeta function.[35]

The second term, labeled I_{AP}^{stim}, contains all the magnon occupation numbers and it represents absorption and stimulated emission processes,

$$
\begin{aligned}
I_{AP}^{\mathrm{stim}}=&-\frac{e}{h}\frac{1}{2\xi\mathcal{N}}\int_{-\infty}^{+\infty}d\epsilon\int_0^{\infty}d\omega\ \Omega(\omega)\{[n_L(\epsilon)\\
&-n_R(\epsilon-eV+\omega)][\mathcal{T}_{++}N_L(\omega)+\mathcal{T}_{--}N_R(\omega)]\\
&+[n_L(\epsilon)-n_R(\epsilon-eV-\omega)]\\
&\times[\mathcal{T}_{++}N_R(\omega)+\mathcal{T}_{--}N_L(\omega)]\}.
\end{aligned}
\tag{22}
$$

It vanishes in the limit of zero temperature on both sides of the junction, but is nonzero for zero bias voltage in the presence of a temperature difference. I_{AP}^{stim} may be written explicitly for arbitrary bias voltage and temperatures,

$$
\begin{aligned}
I_{AP}^{\mathrm{stim}}=&\frac{e}{h}\frac{3}{4\xi\omega_D^{3/2}}\left\{eV(\mathcal{T}_{++}+\mathcal{T}_{--})\Gamma\left(\frac{3}{2}\right)\zeta\left(\frac{3}{2}\right)[(k_BT_L)^{3/2}\right.\\
&+(k_BT_R)^{3/2}]-(\mathcal{T}_{++}-\mathcal{T}_{--})\Gamma\left(\frac{5}{2}\right)\zeta\left(\frac{5}{2}\right)[(k_BT_L)^{5/2}\\
&\left.-(k_BT_R)^{5/2}]\right\}.
\end{aligned}
\tag{23}
$$

D. Calculation of the thermopower

The thermopower S_{AP} is determined by setting the total current to zero, $I_{AP}^{(1)}+I_{AP}^{\rm spont}+I_{AP}^{\rm stim}=0$, and finding the voltage V induced by the temperature difference ΔT, $S_{AP}=-V/\Delta T$. In general we find

$$S_{AP}=-\frac{k_B}{e}\frac{C(\mathcal{T}_{++}-\mathcal{T}_{--})\,\delta m(T)}{[\mathcal{T}_{+-}+\mathcal{T}_{-+}+B(\mathcal{T}_{++}+\mathcal{T}_{--})\,\delta m(T)]}. \tag{24}$$

This is the main result of the paper, describing junctions between ferromagnets of arbitrary polarization strength ranging from weak ferromagnets to half-metals. The factors C and B are dependent on the ratio $\Delta T/T$. We evaluate them in the limits of small, $\Delta T\ll T$, and large, $\Delta T=T_L=T$, $T_R=0$, temperature differences:

$$C=\frac{\zeta\left(\frac{5}{2}\right)}{\zeta\left(\frac{3}{2}\right)}\times\begin{cases}15/8, & \Delta T\ll T,\\ 3/4, & \Delta T=T,\end{cases} \tag{25}$$

$$B=\begin{cases}3/2, & \Delta T\ll T,\\ (3-\sqrt{2})/2, & \Delta T=T.\end{cases} \tag{26}$$

The function $\delta m(T)$ in Eq. (24) is the change in the magnetization due to thermal magnons at temperature T (Bloch's $T^{3/2}$ law),[36]

$$\delta m(T)=\frac{1}{\xi\mathcal{N}}\int_0^\infty d\omega\;\;\Omega(\omega)N_L(\omega)$$
$$=\frac{3}{2\xi}\Gamma\left(\frac{3}{2}\right)\zeta\left(\frac{3}{2}\right)\left(\frac{k_BT}{\omega_D}\right)^{3/2}. \tag{27}$$

The thermopower is finite because the current $I_{AP}^{\rm stim}$ contains a term [last line in Eq. (23)] that depends on the temperature difference. It arises from the difference in the thermal distribution of magnons $N_L(\omega)-N_R(\omega)$ and the process of thermal equilibration between two baths of magnons held at different temperatures, which is mediated by electrons, results in a current. The origin of the factor $\mathcal{T}_{++}-\mathcal{T}_{--}$ in the numerator of Eq. (24) can be understood in the following way. In the electron processes in Fig. 2, which contribute to $\mathcal{T}_{++}$, an increase in the number of magnons in one electrode is achieved by accepting electrons from the other electrode. On the other hand, in the hole processes in Fig. 3, which contribute to $\mathcal{T}_{--}$, an increase in the number of magnons in one electrode is achieved by injecting electrons into the other electrode. Hence the contributions of $\mathcal{T}_{++}$ and $\mathcal{T}_{--}$ proportional to ΔT in the current Eq. (23) appear with opposite signs.

The sign of the thermopower, Eq. (24), is specified for electron (charge $-e$) transfer processes and under the assumption that the exchange between conduction band and core electrons has a ferromagnetic sign. For antiferromagnetic exchange, the overall sign of the thermopower would be opposite. For example, processes (i) and (ii) in Fig. 2 would involve magnons on the opposite side of the junction; hence the current $I_{AP}^{(\rm i,ii)}$ would be determined by magnon occupation numbers $N_{\rm L}(\mathbf{q})$. Note also that we considered a bulk, three-dimensional magnon density of states, but in general the magnitude and sign of the thermopower will depend on the magnon spectrum.

1. Uniformly transparent interface

We model different types of interface by introducing a dependence of the tunneling matrix elements $t_{\mathbf{k_L},\mathbf{k_R}}$ on the wave vectors $\mathbf{k}_L=(\mathbf{k}_L^{||},k_L^z)$ and $\mathbf{k}_R=(\mathbf{k}_R^{||},k_R^z)$, where $\mathbf{k}_{L(R)}^{||}$ is the component parallel to the interface and $k_{L(R)}^z$ is the perpendicular component. For a uniformly transparent interface of area A such that the parallel component of momentum is conserved, we set the dimensionless tunneling factor, Eq. (8), equal to

$$|\tilde{t}_{\mathbf{k_L^{||}},\mathbf{k_R^{||}}}|^2=|t|^2\delta_{\mathbf{k_L^{||}},\mathbf{k_R^{||}}}, \tag{28}$$

so that

$$\mathcal{T}_{\alpha\alpha'}\approx4\pi^2|t|^2\frac{A}{h^2}\min\{\Pi_\alpha,\Pi_{\alpha'}\}, \tag{29}$$

where t represents the transparency of the interface and Π_α is the area of the maximal cross section of the Fermi surface of spins α, $\Pi_+>\Pi_->0$. Then $\mathcal{T}_{+-}=\mathcal{T}_{-+}=\mathcal{T}_{--}=4\pi^2|t|^2(A\Pi_-/h^2)$ and $\mathcal{T}_{++}=4\pi^2|t|^2(A\Pi_+/h^2)$. In the regime $1\gg(1+\Pi_+/\Pi_-)\;\delta m(T)$, the thermopower, Eq. (24), simplifies as

$$S_{AP}=-C\frac{k_B}{e}\frac{(\Pi_+-\Pi_-)}{2\Pi_-}\;\delta m(T). \tag{30}$$

2. Diffusive tunnel barrier

We use a model[34] for describing a strongly nonuniform interface which is transparent in a finite number of points only, randomly distributed over an area A. Each transparent point is treated as a defect which causes electron scattering in the plane parallel to the interface and the tunneling matrix element is a matrix element of the total scattering potential determined with the use of plane waves,

$$\tilde{t}_{\mathbf{k}_L^{||},\mathbf{k}_R^{||}}=\frac{a}{A}\sum_j\;t_j\exp[i\hbar^{-1}(\mathbf{k}_L^{||}-\mathbf{k}_R^{||})\cdot\mathbf{r}_j], \tag{31}$$

where $\mathbf{r}_j$ is the position of the jth contact with area $a\sim\lambda_F^2$. A product of two tunneling matrix elements, averaged with respect to the position of each defect, will be large only if the total phase shift is zero which corresponds to scattering from the same defect,

$$\langle|\tilde{t}_{\mathbf{k_L^{||}},\mathbf{k_R^{||}}}|^2\rangle=\left(\frac{a}{A}\right)^2|t|^2, \tag{32}$$

where a/A accounts for a reduced effective area and $|t|^2=\Sigma_j|t_j|^2$ is an effective transparency. This means that

$$\mathcal{T}_{\alpha\alpha'} \approx 4\pi^2|t|^2\left(\frac{a\Pi_\alpha}{h^2}\right)\left(\frac{a\Pi_{\alpha'}}{h^2}\right). \quad (33)$$

We assume that the densities of states in the spin band α are equal on both sides of the junction so that $\mathcal{T}_{+-}=\mathcal{T}_{-+}$. In the regime $1 \gg (\Pi_+/\Pi_- + \Pi_-/\Pi_+)\ \delta m(T)$, the thermopower Eq. (24) simplifies as

$$S_{AP} = -C\frac{k_B}{e}\frac{(\Pi_+^2 - \Pi_-^2)}{2\Pi_+\Pi_-}\ \delta m(T). \quad (34)$$

III. THERMOPOWER OF A PARALLEL JUNCTION

For parallel orientation of the magnetic polarizations of the ferromagnets, we find that the contribution of magnon-assisted tunneling to the thermopower is zero (upto the lowest order in the electron-magnon interaction). We consider the majority electrons on both sides of the junction to be spin up and the minority electrons to be spin down, and the technical details of the calculation of the current are similar to those described previously for the antiparallel orientation. There is a first-order, elastic contribution $I_P^{(1)}$,

$$I_P^{(1)} \approx \frac{e^2}{h}V(\mathcal{T}_{++}+\mathcal{T}_{--}) + \mathcal{O}\left(\frac{e}{h}\frac{k_B^2 T\Delta T}{\epsilon_F}\right), \quad (35)$$

involving tunneling between majority states on the left and right, $\mathcal{T}_{++}$, and tunneling between minority states, $\mathcal{T}_{--}$, without any spin-flip processes. The first term in Eq. (35) corresponds to a large current response to finite voltage whereas the second term arises from the energy dependence of the electronic density of states near the Fermi energy.

To the lowest order in the electron-magnon interaction there are eight magnon-assisted tunneling processes which are shown schematically in Fig. 4. The top four processes (i)–(iv) involve transitions between minority states on the left and majority states on the right, whereas the lower four processes (v)–(viii) involve transitions between majority states on the left and minority states on the right. The overall contribution to the thermopower is zero because the stimulated emission part of the current does not depend on the temperature difference across the junction,

$$I_P^{\text{stim}} = \frac{e}{h}\frac{3}{4\xi\omega_D^{3/2}}\Bigg\{eV(\mathcal{T}_{+-}+\mathcal{T}_{-+})\Gamma\left(\frac{3}{2}\right)\zeta\left(\frac{3}{2}\right)[(k_BT_L)^{3/2} + (k_BT_R)^{3/2}] - (\mathcal{T}_{+-}-\mathcal{T}_{-+})\Gamma\left(\frac{5}{2}\right)\zeta\left(\frac{5}{2}\right)[(k_BT_L)^{5/2} + (k_BT_R)^{5/2}]\Bigg\}. \quad (36)$$

This can be understood by examining the processes in Fig. 4. The top four processes (i)–(iv), which have minority states on the left and majority on the right, all produce terms proportional to $\mathcal{T}_{-+}$. Two of them, (i) and (ii), are electron-type processes in which an increase (decrease) in the number of magnons on the right is achieved by accepting (injecting) electrons from (into) the left, but the other two (iii) and (iv) are hole-type processes in which an increase (decrease) in the number of magnons on the left is achieved by injecting (accepting) electrons into (from) the right. Therefore the term proportional to $\mathcal{T}_{-+}$ in the last line of I_P^{stim}, Eq. (36), does not depend on the temperature difference but a sum $(k_BT_L)^{5/2}+(k_BT_R)^{5/2}$. The same is true for the lower four processes in Fig. 4, (v)–(viii), which produce terms proportional to $\mathcal{T}_{+-}$.

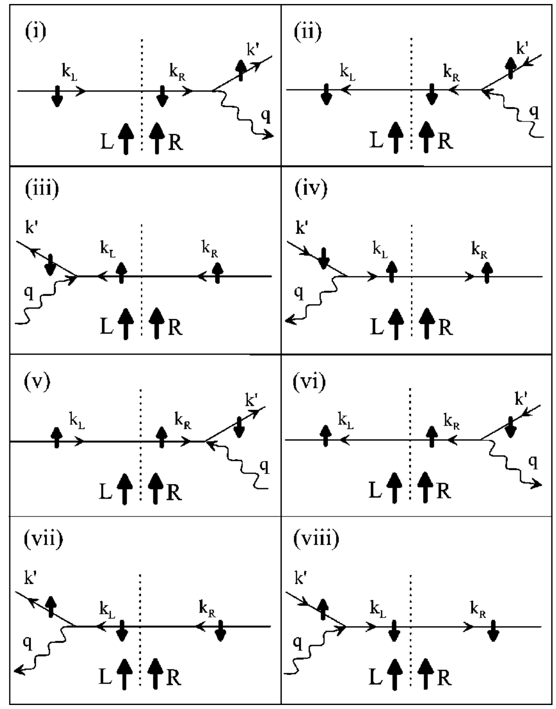

FIG. 4. Schematic of magnon-assisted tunneling across a junction with ferromagnetic electrodes in the parallel configuration. Eight processes which, to lowest order in the electron-magnon interaction, contribute to magnon-assisted tunneling. (i)–(iv) involve transitions between minority states on the left and majority states on the right via a virtual intermediate state. (v)–(viii) involve transitions between majority states on the left and minority states on the right via a virtual intermediate state.

IV. CONCLUSION

As shown above, the thermopower of a tunnel F-F junction in the parallel configuration, $S_P \sim k_B^2 T/(e\epsilon_F)$, is smaller than the contribution of magnon-assisted transport to the thermopower S_{AP} in the antiparallel configuration, Eq. (1). As the relative polarizations of ferromagnetic layers can be manipulated by an external magnetic field, the large difference $\Delta S = S_{AP} - S_P$ results in a magnetothermopower effect. As a rough estimate, we take $\epsilon_F = 5$eV and $\delta m = 7.5 \times 10^{-6}\ T^{3/2}$ (for a ferromagnet such as Ni, Ref. 36) to give $S_{AP} \sim -3\ \mu\text{V}\,\text{K}^{-1}$ and $S_P \sim 0.5\ \mu\text{V}\,\text{K}^{-1}$ at $T = 300$ K.

As an extreme example, we predict a giant magnetothermopower for a junction between two half-metallic ferromagnets. In a half-metal the splitting Δ between the majority and minority conduction bands is greater than ϵ_F measured from the bottom of the majority band so that only majority carriers are present at the Fermi energy. In this case $\mathcal{T}_{+-}=\mathcal{T}_{-+}=\mathcal{T}_{--}=0$ in Eq. (24) and, in the linear regime $\Delta T \ll T_L$,

$$S_{AP}=-0.64\frac{k_B}{e}, \quad S_P\sim\frac{k_B^2 T}{e\epsilon_F}. \tag{37}$$

This result is independent of temperature and of the specific half-metallic material, and it represents a giant magnetothermopower effect $\Delta S\approx S_{AP}\approx -55\ \mu\mathrm{V\,K}^{-1}$.

A strong polarization dependence of the thermopower, $\Delta S\approx S_{AP}$, enables one to separate the interface contribution to the thermopower from effects arising from a finite-temperature gradient in the reservoirs. We assume in our analysis that phonon-mediated heat conduction is much lower than the electronic one and that a fast temperature equilibration inside the ferromagnetic metal makes a finite-temperature drop across the tunnel barrier possible. Furthermore, the predicted interface magnetothermopower will be most pronounced in a geometry where the bottleneck for electron transport is also the bottleneck for thermal transport: in a small-area mesoscopic junction, ideally, in a suspended scanning-tunneling-microscope-type (STM-type) geometry.

ACKNOWLEDGMENTS

The authors thank A. Geim, C. Marrows, I. Mazin, and G. Tkachov for discussions. This work was supported by EPSRC, the Royal Society, and the EU High Field Infrastructure Cooperative Network.

[1] G.A. Prinz, Phys. Today **48** (4), 58 (1995); Science **282**, 1660 (1998), and references therein.
[2] M. Julliere, Phys. Lett. **54A**, 225 (1975).
[3] J.S. Moodera, T.H. Kim, C. Tanaka, and C.H. de Groot, Philos. Mag. B **80**, 195 (2000).
[4] M.N. Baibich, J.M. Broto, A. Fert, N. Van Dau, F. Petroff, P. Eitenne, G. Creuzet, A. Friederich, and J. Chazelas, Phys. Rev. Lett. **61**, 2472 (1988); G. Binasch, P. Grünberg, F. Saurenbach, and W. Zinn, Phys. Rev. B **39**, 4828 (1989).
[5] W.P. Pratt, Jr., S.F. Lee, J.M. Slaughter, R. Loloee, P.A. Schroeder, and J. Bass, Phys. Rev. Lett. **66**, 3060 (1991); S.F. Lee, W.P. Pratt, Jr., R. Loloee, P.A. Schroeder, and J. Bass, Phys. Rev. B **46**, 548 (1992).
[6] J. Sakurai, M. Horie, S. Araki, H. Yamamoto, and T. Shinjo, J. Phys. Soc. Jpn. **60**, 2522 (1991).
[7] M.J. Conover, M.B. Brodsky, J.E. Mattson, C.H. Sowers, and S.D. Bader, J. Magn. Magn. Mater. **102**, L5 (1991).
[8] L. Piraux, A. Fert, P.A. Schroeder, R. Loloee, and P. Etienne, J. Magn. Magn. Mater. **110**, L247 (1992).
[9] E. Avdi, B.J. Hickey, D. Greig, M.A. Howson, M.J. Hall, J. Xu, M.J. Walker, N. Wiser, and P. de Groot, J. Appl. Phys. **73**, 5521 (1993).
[10] J. Shi, R.C. Yu, S.S.P. Parkin, and M.B. Salamon, J. Appl. Phys. **73**, 5524 (1993).
[11] L. Piraux, M. Cassart, J.S. Jiang, J.Q. Xiao, and C.L. Chien, Phys. Rev. B **48**, 638 (1993).
[12] J. Shi, E. Kita, L. Xing, and M.B. Salamon, Phys. Rev. B **48**, 16 119 (1993).
[13] J. Shi, K. Pettit, E. Kita, S.S.P. Parkin, R. Nakatini, and M.B. Salamon, Phys. Rev. B **54**, 15 273 (1996).
[14] H. Sato, S. Miya, Y. Kobayashi, Y. Aoki, H. Yamamoto, and M. Nakada, J. Appl. Phys. **83**, 5927 (1998).
[15] S.A. Baily, M.B. Salamon, and W. Oepts, J. Appl. Phys. **87**, 4855 (2000).
[16] M. Johnson and R.H. Silsbee, Phys. Rev. B **35**, 4959 (1987).
[17] J. Ziman, *Principles of the Theory of Solids* (Cambridge University Press, Cambridge, England, 1964).
[18] E.Yu. Tsymbal, D.G. Pettifor, J. Shi, and M.B. Salamon, Phys. Rev. B **59**, 8371 (1999).
[19] A.M. Bratkovsky, Appl. Phys. Lett. **72**, 2334 (1998); A.H. MacDonald, T. Jungwirth, and M. Kasner, Phys. Rev. Lett. **81**, 705 (1998); F. Guinea, Phys. Rev. B **58**, 9212 (1998).
[20] D.C. Tsui, R.E. Dietz, and L.R. Walker, Phys. Rev. Lett. **27**, 1729 (1971); J.S. Moodera, J. Nowak, and R.J.M. van de Veerdonk, *ibid.* **80**, 2941 (1998).
[21] E. McCann and V. I. Fal'ko (unpublished).
[22] M.H. Cohen, L.M. Falicov, and J.C. Phillips, Phys. Rev. Lett. **8**, 316 (1962).
[23] C. Caroli, R. Combescot, P. Nozieres, and D. Saint-James, J. Phys. C **4**, 916 (1971).
[24] G. D. Mahon, *Many-Particle Physics* (Plenum, New York, 1981).
[25] R.B. Woolsey and R.M. White, Phys. Rev. B **1**, 4474 (1970); B.S. Shastry and D.C. Mattis, Phys. Rev. B **24**, 5340 (1981); S.R. Allan and D.M. Edwards, J. Phys. C **15**, 2151 (1982); M.I. Auslender and V.Y. Irkhin, *ibid.* **18**, 3533 (1985).
[26] E.L. Nagaev, Phys. Status Solidi B **65**, 11 (1974); W. Nolting, *ibid.* **96**, 11 (1979).
[27] D.M. Edwards and J.A. Hertz, J. Phys. F: Met. Phys. **3**, 2174 (1973); **3**, 2191 (1973).
[28] T. Holstein and H. Primakoff, Phys. Rev. **58**, 1048 (1940).
[29] R. P. Feynman and A. R. Hibbs, *Quantum Mechanics and Path Integrals* (McGraw-Hill, New York, 1965).
[30] R. Landauer, Philos. Mag. **21**, 863 (1970).
[31] D.S. Fisher and P.A. Lee, Phys. Rev. B **23**, 6851 (1981).
[32] C.W.J. Beenakker, Rev. Mod. Phys. **69**, 731 (1997).
[33] E. McCann and V.I. Fal'ko, Europhys. Lett. **56**, 583 (2001).
[34] G. Tkachov, E. McCann, and V.I. Fal'ko, Phys. Rev. B **65**, 024519 (2002).
[35] I. S. Gradshteyn and I. M. Ryzhik, *Table of Integrals, Series, and Products* (Academic Press, San Diego, 1965).
[36] C. Kittel, *Introduction to Solid State Physics* (Wiley, New York, 1996).